ACS APPLIED MATERIALS & INTERFACES

Research Article

www.acsami.org

Formation of Three-Dimensional Ordered Hierarchically Porous Metal Oxides via a Hybridized Epoxide Assisted/Colloidal Crystal Templating Approach

Marauo Davis, Donald A. Ramirez, and Louisa J. Hope-Weeks*

Department of Chemistry and Biochemistry, Texas Tech University, Lubbock, Texas 79409, United States

Supporting Information

ABSTRACT: Three-dimensionally ordered hierarchically porous alumina, iron(III) oxide, yttria, and nickel oxide have been prepared through the hybridization of colloidal crystal-templating and a modified sol−gel method. Simply, highly ordered arrays of poly(methyl methacrylate) (PMMA) were infiltrated with a precursor solution of metal salt and epoxide. Calcination after solidification of the material removed the polymer template while forming the inverse replicas, simultaneously. These hierarchical structures possessing macropore windows and mesopore walls were characterized by powder X-ray diffraction (PXRD), thermogravimetric analysis (TGA), scanning electron microscopy (SEM), and N_2 adsorption/desorption techniques to probe the structural integrity. It was revealed by PXRD that the prepared 3D frameworks were single-phase polycrystalline structures with grain sizes between 5 and 27 nm. The thermal stability as studied by TGA illustrates expected weight losses and full decomposition of the PMMA template. SEM reveals the bimodal, hierarchical macroporous frameworks with well-defined macropore windows and mesoporous walls. Gas sorption measurements of the ordered materials display surface areas as high as 93 $m^2 g^{-1}$, and average mesopore diameter up to 33 nm. Due to the versatility of this method, we expect these materials will be ideal candidates for applications in catalysis, adsorption, and separations. Furthermore, the implementation of this technology for production of three-dimensionally ordered macroporous materials can improve the cost and efficiency of metal oxide frameworks (MOFs) due to its high versatility and amenability to numerous systems.

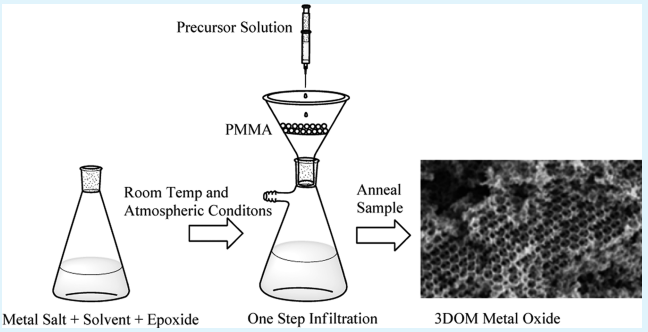

KEYWORDS: *epoxide addition, three-dimensional macropores, metal oxide, colloidal crystal templating, hierarchical materials*

INTRODUCTION

Inverse opals are three dimensionally ordered macroporous (3DOM) materials that have received vast attention in recent years due to their applications in the field of catalysis, optics, separation, and sensing.[1−7] These hierarchical macroporous assemblies are typically prepared via a colloidal crystal templating approach, that generates well-ordered, periodic pore structures.[2] Colloidal crystal templating is a hard-templating method in which the produced porosity is the direct product of a precursor solution having solidified in the interstitial void spaces of the host material.[6] The most commonly employed colloidal crystals have been those of face-centered cubic (fcc) arrangements of monodispersed spheres, typically polystyrene (PS) and poly(methyl methacrylate) (PMMA). After the precursor has solidified around the spheres, the polymer template is removed either by calcination or extraction. This processing technique leads to the formation of 3DOMs possessing high porosity consisting of bimodal distribution of meso/macropores and high surface areas.[8]

For some time, the most popular synthetic method for the production of 3DOM metal oxides was an alkoxide-based strategy.[3,4] However, the expensive costs associated with the production of organometallic precursors hampers the attraction to scale up using these materials. Additionally, this approach is limited due to availability and diversity of metal alkoxides commercially obtainable and by the lack of stability with respect to hydrolysis of many transition metal alkoxides, these factors have combined to limit the diversity of materials produced by this method. This approach is also limited when applied to forming complex oxide structures where the differing rates of hydrolysis of the metal alkoxide precursors results in the formation of materials that lack chemical homogeneity.[9] These disadvantages have required chemist to look for alternative methods for preparation of 3DOM metal oxides. It was not until several years ago that Yan et al. introduced a more facile method which has the advantage of infiltrating with much

Received: April 25, 2013
Accepted: July 19, 2013
Published: August 8, 2013

cheaper and more readily available metal acetates and nitrates into ordered, PS spheres' voids, followed by vacuum filtration to remove excess solution and then drying in an oven.[10] From there the dried material is soaked in oxalic acid for 5−10 min followed by another round of vacuum filtration and drying.[10] The metal oxalate could then be converted into the corresponding metal oxide by means of calcination. This technique set the groundwork for incorporating cheap metal salts as precursors for this sol−gel process.[11−13] While this method has been shown to be highly versatile and can be used to incorporate a diverse range of metals, it often requires time-consuming multistep process to achieve successful infiltration of the metal precursors.[10] This oxalate method has been further modified by Ueda et al. reducing the number of steps and no longer requiring oxalic acid for polymerization and instead relies on *in situ* nitrate oxidation for sol−gel formation.[13] This system has the advantage of producing mixed metal oxides with a controlled metal ratio. However, the solvent system is restricted to a mixture of ethylene glycol−methanol in this method, which ultimately limits the diversity of metal nitrates that can be utilized to form the metal oxide.[14]

Since the development of this approach, other groups have focused on a "dual templating" method (using both soft and hard) to prepare 3DOM frameworks with high surface areas and crystalline mesoporous walls with large pore volumes.[5,15] For example, these processes employ a triblock copolymer like Pluronic F127 or P123 as an additive to the starting solution to enhance the surface area of the final product.

Researchers have been able to gather a more thorough understanding of synthetic pathways and tunability of morphology in 3DOM synthesis.[11,16−18] Despite their many contributions, some fundamental issues still exist, perhaps the most pressing are "scale-up/fast production", applicability to a variety of metal systems, and cost.[19] Choice of metals, length and number of steps, operation conditions, and controllability are important factors if commercialization is the ultimate goal. With these requirements in mind and our group's extensive work using epoxide assisted sol−gel chemistry, this technique was combined with the hard-templating technique to produce 3DOM materials.

To this end, we report, for the first time, use of the epoxide-assisted sol−gel method for the preparation of 3DOM hierarchical metal oxides through colloidal crystal templating with PMMA. Through extensive investigation of the epoxide method, we have gained knowledge of the subtle synthetic changes and parameters by which to tune a materials' architecture and speed of sol−gel formation by adjusting the type of metal salt and its concentration, epoxide, temperature, and/or solvent used.[20−22] The importance of having this ability to control and tune the structure is demonstrated in materials for supercapacitors, electrocatalyst, semiconductors, and support catalyst where the chemical composition, particle size, particle morphology, defect concentration, crystallinity, and surface area determine the functionality of the material.[22] One can see that with all of these characteristics playing an important role in the physical properties of the material, a highly tailorable synthetic methodology is valuable for incorporation into preparing 3DOM materials and provides new benefits that previous methods lacked. It is well-documented that the epoxide-assisted approach is highly versatile in the preparation of numerous mesoporous metal oxide frameworks.[20,22−26] This method, first reported by Gash et al., is different from other sol−gel methods in that it uses an organic epoxide with metal salts for sol−gel polymerization and therefore forms different molecular species than the alkoxide method.[27] In this preparative technique, an inorganic metal nitrate or halide salt acts as the weak acid in an aqueous or alcoholic solution, and the epoxide, acting as the acid scavenger, accepts a proton from the hydrated metal species, raising the solution pH moderately and uniformly allowing growth of metal hydroxide/oxide species through a series of olation and oxolation reactions.[26,28] Simultaneously in solution, the protonated epoxide is consumed through an irreversible ring-opening reaction by the counterion.[28] This sol−gel technique has proven to be advantageous for fabricating various metal oxides with desired surface properties and morphologies, while also being a dynamic methodology as shown by the ability to make 15 different composite systems of metal oxide/silicon oxide systems using the same synthetic method thus demonstrating the versatility of the method.[29,30] An example of material prepared using the epoxide method is aluminum doped Fe_2O_3 as used as an energetic material which has the advantage of producing materials with higher purity, homogeneity, and safety over traditional preparative techniques.[31] Another example is the creation of crystalline iron oxide aerogels with mesoporous magnetic architecture, this material with superparamagnetic properties is a result of modifying pore-solid architecture and the FeO_x nanocrystalline phase, the ability to control this was done by manipulating synthetic and process conditions.[32] Potassium-doped iron oxide aerogels and xerogels prepared by the epoxide method were shown to be active for Fischer−Tropsch synthesis of diesel fuel.[33] Additionally, the robust and multifaceted nature of this process is critical for the mass production of main group, transition, and rare earth metal oxides.[23,30,34−36]

Herein, we report the synthesis of macroporous alumina, iron(III) oxide, yttria, and nickel oxide with mesoporous walls via integration of the well-established epoxide assisted method and colloidal crystal templating with PMMA spheres. This paper illustrates the idea that a process originally designed to prepare mesoporous materials can be extended to fabricating three-dimensionally ordered macroporous networks. Furthermore, this report demonstrates the preparation of interesting metal oxides of Al, Fe, Y, and N, which as oxides have previously been used in applications, in order to establish the scope of this general method. The synthetic design used, here, illustrates the idea that a true mesoporous network can be established through a "one-pot" approach without use of a secondary template. The requirements, steps, and limitations using this hybridized method are few when compared to other techniques for making 3DOM structures. However the variety of materials that could be made using this technique makes it quite attractive as previously inaccessible materials can now be prepared. For the first time, pure yttria 3DOM structure has been prepared as a result of using the epoxide assisted method demonstrating the benefit of this new hybridized method. Optimal conditions and structural features of these materials have been detailed and characterized by powder X-ray diffraction (PXRD), thermogravimetric analysis (TGA), scanning electron microscopy (SEM), and gas sorption techniques.

EXPERIMENTAL SECTION

Materials. Methyl methacrylate (MMA) (stabilized, 99%), 2,2′-azobis(2-methylpropionamidine)dihydrochloride, deionized water, aluminum(III) nitrate nonahydrate, iron(III) nitrate nonahydrate, yttrium(III) chloride hexahydrate, nickel(II) chloride hexahydrate,

absolute ethanol, and propylene oxide were all used as received without further purification.

Synthesis of PMMA Colloidal Crystals. Suspensions of monodisperse poly(methyl methacrylate) (PMMA) spheres (diameter, 303 ± 15 or 369 ± 21 nm) were prepared following literature techniques and packed into colloidal crystals via centrifugation.[4] In detail, deionized water (1.6 L) and MMA (300 or 400 mL for larger spheres) were added to a 3-necked round-bottomed flask (3000 mL in volume) equipped with a mechanical stirrer (glass shaft with Teflon stirrer blade), water-cooled reflux condenser with slow nitrogen flow, and a thermocouple probe. This mixture was then stirred (∼350 rpm) while being heated to 80 °C (70 °C for larger spheres). After the reaction mixture was stabilized for 15 min, the azo initiator (1.5 g) was added and the polymerization reaction was started. The reaction temperature was then maintained for 1 h with the colloidal suspension turning milky white after a few minutes. After the polymerization was completed, the round-bottomed flask was stoppered, placed on a cork stand, and permitted to cool for 1 h. The resulting colloidal PMMA spheres were then filtered through glass wool to remove large agglomerates. The PMMA was packed via centrifugation at 1500 rpm for 24 h. Afterward, the supernatant was decanted, and the bulk solid was permitted to dry at ambient conditions for ∼1 week. The PMMA colloidal crystals were lightly crushed to form a powder before use. Two types of PMMA spheres were used in these syntheses with diameters of 303 ± 15 and 369 ± 21 nm, as measured by scanning electron microscopy (SEM) (see Supporting Information Figures S1 and S2).

Fabrication of 3DOM Alumina. Hierarchical porous alumina was prepared by the following procedure: PMMA powder was added to filter paper previously wetted with ethanol over vacuum on a Büchner funnel. The PMMA was then evenly spread over the filter paper. Afterward, 10 mL of $Al(NO_3)_3{\cdot}9H_2O$ (0.62 M, ethanolic solution) was slowly added to a vial followed by the addition of 11 equiv of propylene oxide (in two equal portions), mixed thoroughly and then allowed to stand 1−3 min before infiltration. Then, with suction applied, the precursor solution was added dropwise until it completely covered the PMMA spheres. Equal amounts, by mass, of PMMA and precursor solution were used. The sample was then permitted to dry over vacuum for approximately 5 min and then removed and permitted to dry at room temperature for 24 h. The PMMA template was then removed via calcination in static air by heating from 25 to 300 °C (2 °C min^{-1}), dwelling for 3 h, and then further heating to 800 °C (2 °C min^{-1}), dwelling for 2 h, before returning to 25 °C (10 °C min^{-1}). Alumina samples were prepared from PMMA spheres with average diameters of 303 ± 15 nm.

Synthesis of Macroporous Iron(III) Oxide and Yttria. Macroporous iron(III) oxide or yttria were prepared by the same procedure as macroporous alumina except that a 0.46 M ethanolic stock solution of $Fe(NO_3)_3{\cdot}9H_2O$ or $YCl_3{\cdot}6H_2O$ was used for iron(III) oxide and yttria, respectively. In the preparation of iron(III) oxide, the reaction proceeded very quickly. Therefore, immediately after the addition of propylene oxide and brief mixing, the solution was added evenly over the PMMA template within 1 min. In the case of yttria, gelation proceeded slowly allowing 10−12 min before infiltration. For template removal, the temperature and ramping rate for calcination was held constant from ambient to 300 °C (2 °C min^{-1}) to first remove the PMMA template. However, in this case, the phase pure metal oxide was formed by increasing temperature up to 400 or 600 °C (2 °C min^{-1}), for Fe_2O_3 and Y_2O_3, respectively, and then dwelling for 3 h before returning to room temperature (10 °C min^{-1}). Fe_2O_3 samples were prepared from PMMA spheres with average diameters of 369 ± 21 nm while yttria samples were prepared from PMMA spheres with average diameters of 303 ± 15 nm.

Fabrication of Macroporous Nickel Oxide. PMMA powder was added to filter paper previously wetted with ethanol over vacuum on a Büchner funnel. The PMMA was then evenly spread over the filter paper. Then, 10 mL of a 0.62 M ethanolic stock solution of $NiCl_2{\cdot}6H_2O$ was added to a vial followed by the addition of 11 equiv of propylene oxide. Once the epoxide was added, the sol was permitted to sit 5−8 min before infiltration. Then, with suction applied, the precursor solution was added over PMMA and finally permitted to dry 5−10 min before removing. The filter paper was then removed and left to dry at room temperature for 24 h prior to annealing. For annealing, the samples were placed in a programmable furnace and heated from 25 to 300 °C (2 °C min^{-1}), dwelling for 3 h, and then further heating to 400 °C (2 °C min^{-1}), dwelling for 6 h, before returning to 25 °C (10 °C min^{-1}). NiO samples were prepared from PMMA spheres with average diameters of 369 ± 21 nm. Equal amounts, by mass, of PMMA and precursor solution were used.

Physical Characterizations. Powder X-ray diffraction (PXRD) patterns of the samples were recorded with a Rigaku Ultima III diffractometer using Cu Kα radiation. To prepare the samples for X-ray powder diffraction, each sample was finely ground, and measurements were taken at a 2θ range of 10−80° at a step-width of 0.03° s^{-1}. PXRD patterns were identified by comparison to the phases in the International Centre for Diffraction Data (ICDD) powder diffraction file (PDF) database. Grain sizes were calculated using Scherrer's equation corrected for line broadening. Thermogravimetric analysis (TGA) profiles were collected on a Shimadzu TG-50 under N_2 from 25 to 600 °C at 10 °C min^{-1}. Scanning electron microscopy (SEM) images were obtained on a Hitachi S-4300. The samples were first mounted on an aluminum stub with carbon tape and then sputter coated with Au to minimize charging effects. The specific surface area, pore volume, and average pore size of each material was obtained from the N_2 adsorption/desorption isotherms obtained at 77 K on a Nova 4200e model Surface Area Analyzer (Quantachrome Instrument Corp.) The Brunauer−Emmett−Teller (BET) specific surface areas were calculated from the adsorption branch of the isotherm, while the average pore diameters, and average pore volumes were all taken from the desorption branch employing the Barrett−Joyner−Halenda (BJH) model. Prior to obtaining any results, the samples were placed on degas for 24 h at 120 °C. Each set of measurements was taken at 77 mm Hg and an equilibrium time of 600 s resulting in a total experimentation time of 9−12 h per sample.

RESULTS AND DISCUSSION

Facile Synthesis of 3DOM Materials. Hierarchical macroporous 3DOM materials of alumina, iron(III) oxide, yttria, and nickel oxide were prepared using a combined colloidal crystal templating/epoxide addition method with propylene oxide as the "gel" initiator. This hybridized approach proceeds in just a few steps: (i) the initial sol is infiltrated into the PMMA template and (ii) then proceeds to solidify in the interstitial space of the colloidal crystal template. Given the knowledge of olation and oxolation reactions that occur in this process, the formed solid is expected to be a $M(OH)_x$ species. The overall quality of the produced macroporous material strongly depends on the completion of the polymerization reactions occurring in the void spaces. For this reason, the materials are dried over vacuum for ∼5 min and then left to dry and "age" under ambient conditions for at least 24 h before calcination. After drying, the PMMA template removal and metal oxide formation occurred via calcination. Obviously, due to the high porosity and thin walls present, these materials are quite fragile. Calcination conditions such as temperature, rate, atmosphere, and dwell time are instrumental in obtaining high quality 3DOM materials.[11]

The Stein group at the University of Minnesota has contributed greatly in this arena by investigating and studying the processing conditions of 3DOMs and discovered that calcination conditions such as temperature, rate, atmosphere, and dwell time are instrumental in obtaining high quality 3DOM materials.[11] For example, heating of the samples to extreme temperatures will result in additional grain growth and densification as a result of Ostwald ripening.[37] To retain an ordered structure, a slow heating rate, typically 2 °C min^{-1},

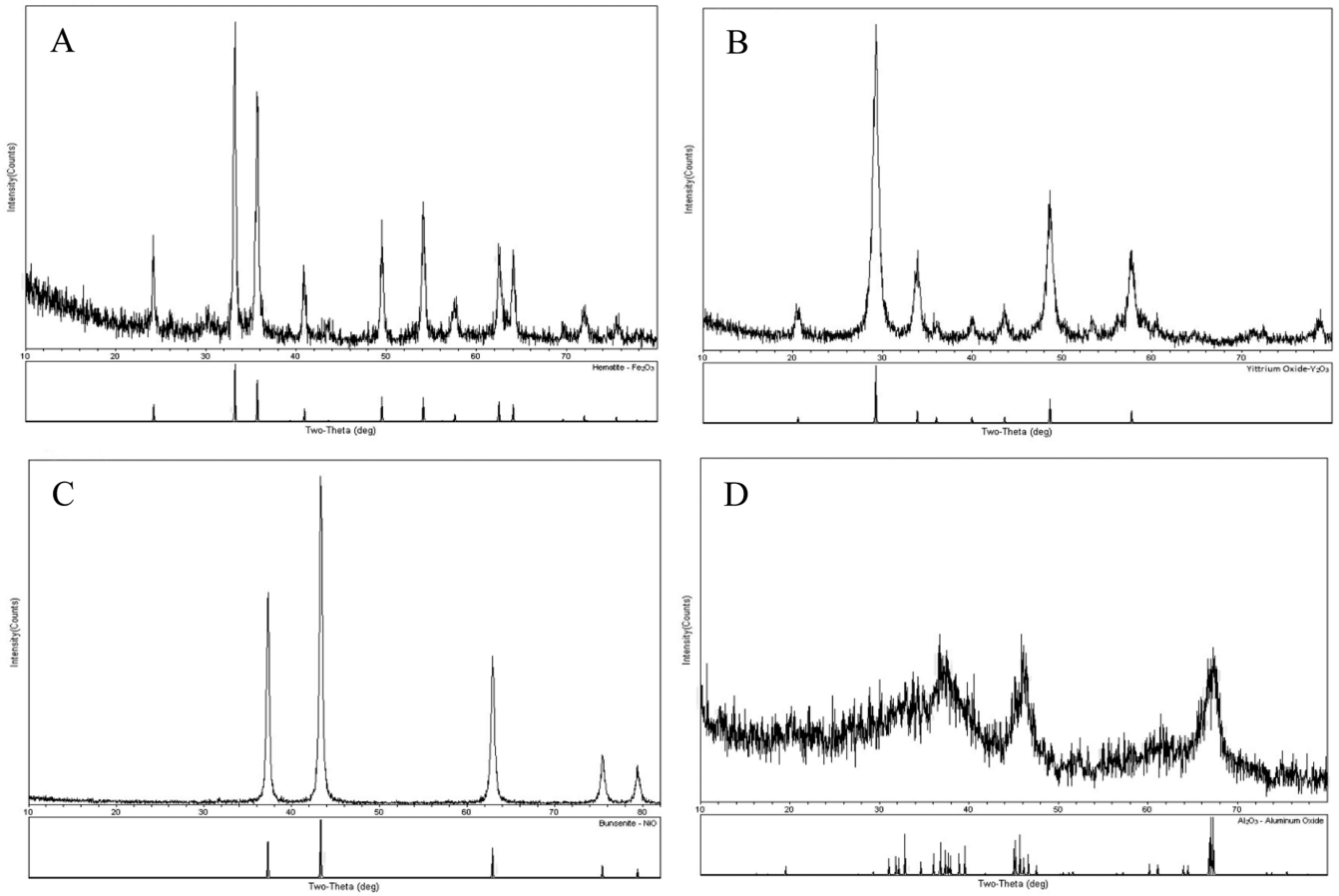

Figure 1. Powder X-ray diffraction patterns of 3DOM samples matched to standards from the ICDD database: (A) Fe_2O_3—hematite; (B) Y_2O_3—yittrium oxide; (C) NiO—bunsenite; (D) Al_2O_3—aluminum oxide.

must be employed to remove the template and minimizes uneven thermal expansion during the annealing process.

Calcination of PMMA in air results in an initial mass loss at 305 °C and reaches full degradation at 370 °C. As a result, for metal oxide formation, all samples were annealed ≥400 °C, with appropriate dwell times, to ensure complete removal of the polymer and formation of the desired metal oxide phase.

Crystal Structure. Powder X-ray diffraction patterns for each formed 3DOM material could be identified as a single, crystalline phase and are represented in Figure 1. Table 1 illustrates the crystal phase, crystallite size, annealing temperatures, and corresponding PDFs for each material of interest.

Table 1 illustrates the crystal phase, crystallite size, annealing temperatures, and corresponding PDFs for each material of interest. Figure 1D shows that, under the conditions reported, alumina is still highly amorphous; however, weak reflections are observed. In contrast, upon annealing, in Figure 1A, several diffraction peaks are illustrated that could all be assigned as belonging to rhombohedral Fe_2O_3. Figure 1B shows the reflections as assigned for cubic yttria, Y_2O_3. And finally, Figure 1C highlights the monoclinic NiO system with the most crystalline (200) plane present at 43°.

Table 1. Crystal Phase and Grain Size Measurements As Determined via PXRD and Calcination Temperatures for 3DOM Samples with Percent Error Listed in Parentheses

case	Al	Fe	Y	Ni
crystal phase	Al_2O_3	Fe_2O_3	Y_2O_3	NiO
crystallite size (nm)	5(0.5)	27(0.94)	11(0.31)	31(0.12)
calcination temperature (°C)	800	400	600	400
PDF no.	47-1308	33-0664	65-3178	65-6920

Thermal Stabiliy. To ensure decomposition and removal of the PMMA template followed by formation of the metal oxide phase, thermal analyses were completed (see Supporting Information Figure S3). In each analysis, an initial weight loss (3–7%) was observed below 270 °C, and this could be best assigned to the removal of absorbed water and residual solvent.[5,38] Collectively, one of two phenomenon was observed in each case: either two distinct weight losses or one large weight loss occurred. For example, in the case of alumina and yttria, two distinct weight losses occurred at ranges 270–320 °C, corresponding to the beginning oxidation and removal of PMMA, and then at 320–450 °C, corresponding to the full decomposition of PMMA and formation of the Al_2O_3 or Y_2O_3 phase.[5,13,20,23] Conversely, both Fe_2O_3 and NiO thermograms revealed one large weight loss occurring at a temperature range of 240–420 °C. From these profiles and knowledge of the corresponding transformation of metal hydroxide species formed via the epoxide addition method, it is suggested that both a $M(OH)_x$ to MO_x and the decomposition of PMMA reaction(s) are occurring simultaneously. In addition, Fe_2O_3 has been shown to form at room temperature and formation of NiO, from this approach, is achievable in the investigated

dx.doi.org/10.1021/am401522n | ACS Appl. Mater. Interfaces 2013, 5, 7786–7792

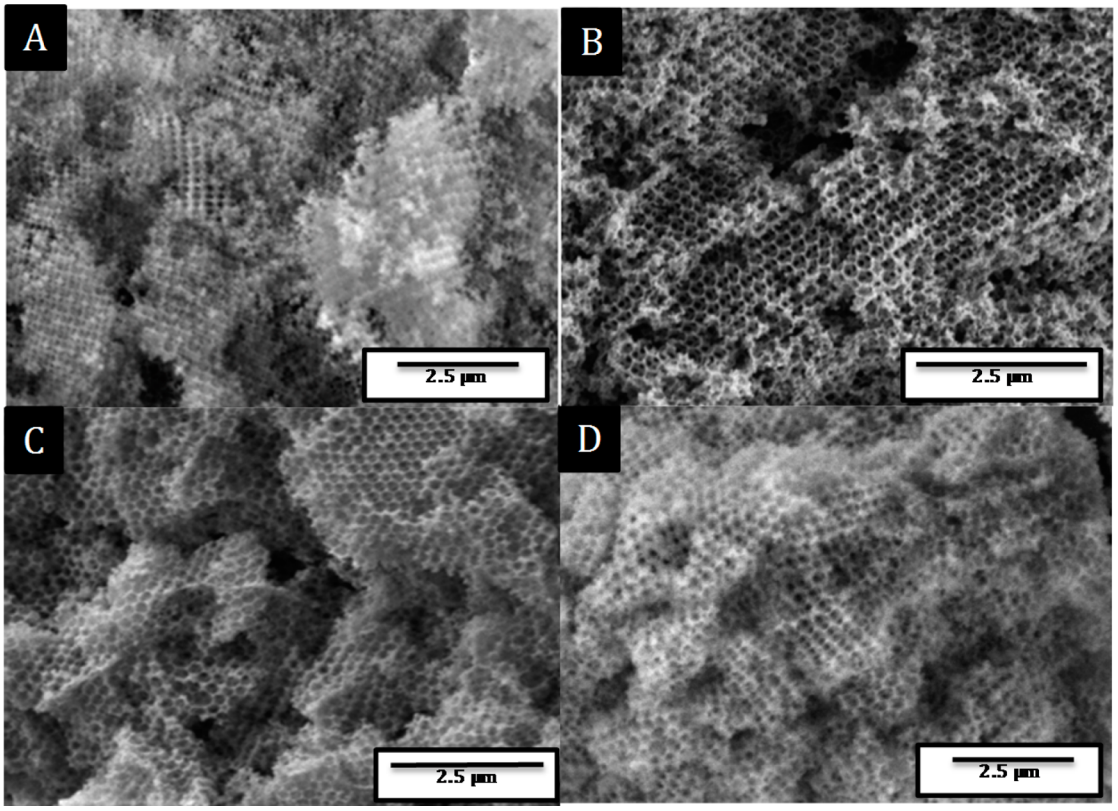

Figure 2. SEM images for macroporous inverse replicas of (A) alumina; (B) Fe_2O_3; (C) Y_2O_3; (D) NiO.

Table 2. Gas Sorption Measurements of 3DOM Materials Including Specific Surface Area, Average Pore Diameters, and Average Pore Volume with Percent Error Listed in Parentheses

case	Al	Fe	Y	Ni
surface area (m^2 g^{-1})	93(3.2)	23(0.6)	36(2.2)	23(1.5)
pore diameter (nm)	21(0.6)	33(0.4)	7(0.5)	8(0.6)
pore volume (mL g^{-1})	0.266(0.014)	0.122(0.003)	0.152(0.009)	0.118(0.003)

temperature range, which might explain the overlapping weight losses observed.[24]

Pore Structure and Morphology. Figure 2A–D reveals the bimodal pore structure of alumina, Fe_2O_3, Y_2O_3, and NiO. Although, the annealing conditions differ with each 3DOM, it is apparent that the closed packed arrangement of the PMMA spheres is retained after calcination. In each case, well-ordered materials were produced with the lighter regions representing the mesoporous walls and the darker areas representing the macroporous windows once occupied by PMMA template. Observing the morphology of all the samples, it was found that Fe_2O_3 and Y_2O_3 formed the most consistent; "honeycomb-type" structures and appear to have the highest degree of long-range order. The consistency of the formation of these 3DOM materials might be due to several factors: (i) full infiltration of the precursor solutions and (ii) quick "gel" formation in the interstitial spacing of the template.

For example, in the case of Fe_2O_3 and Y_2O_3, the precursor solution was added directly to the template due to the quick gelation time. However, in the case of alumina and NiO, the precursor solutions were permitted to stand a few minutes before infiltration to increase viscosity and drive formation of the hydroxide intermediate before infiltration. It can be expected, however, that, if the template were a single-phase, colloidal crystal, a perfect 3DOM structure could be obtained.[10]

Surface Area, Pore Diameter, and Pore Volume. The structural character of the mesoporous wall was investigated by N_2 adsorption measurements (see Table 2), and type II isotherms were observed for all samples. These findings correlate with other work suggesting that the low-pressure portion of the plot signifies that the sample is a nonporous or macroporous absorbent.[10] The hysteresis in the high-pressure portion, however, is indicative of capillary condensation occurring within the mesoporous walls. The average surface areas were found to range from 23 to 93 m^2 g^{-1}, and these values are comparable to the literature values of metal oxides prepared from the metal oxalate method.[5] Moreover, the surface area values obtained here for alumina and Fe_2O_3 greatly exceeds or directly compare to those of previous reports which employ a surfactant as a "structure-directing" agent in dual template approaches.[5,14] These findings further illustrate the viability of this method in formation of high surface area, ordered porous materials.

The high surface areas obtained can be attributed completely to the pure, 3DOM structure since the annealing programs used ensure no surface area contribution/support from residual carbon. These surface area values coincide with average pore diameter ranges of 7–33 nm and pore volumes from 0.118 to 0.266 mL g^{-1}. In addition to the expected hierarchical structures revealed by electron microscopy, gas sorption

measurements further confirm the bimodal microstructure the 3DOM materials possess.

CONCLUSION

Here, we report a facile approach to the fabrication of high quality, 3DOM materials of alumina, iron(III) oxide, yttria, and nickel oxide from a hybridized sol−gel/colloidal crystal templating method. The idea of integrating two simple techniques provides significant benefits over existing procedures to prepare 3DOMs. Formation of the metal hydroxide species, which serves as the mesoporous walls, first, by epoxide addition, ensures high surface areas in the final structure. More than that, advantages to this approach are embodied in the versatility of the epoxide addition method, low cost of starting materials, and amenability for the mass production of various other single and mixed-metal composite frameworks. The epoxide addition method is advantageous over current approaches for the synthesis of ordered macroporous materials.[10,13] For example, this methodology, in combination with colloidal templating, provides a straightforward, scalable approach to the synthesis of 3DOMs. The SEM images indicate that the samples are homogenous and exhibit long-range order that are comparable to other approaches.[10,13] The importance of this method was demonstrated as 3DOM yttria was prepared for the first time. The next reasonable step would be bimetallic and composite systems, taking advantage of the large variety of metals offered using the epoxide method. In theory, the tunability and modulation of surface morphology for specific applications should be easily attainable through subtle synthetic changes.[20−22,39−41] Perhaps, the novelty is that this synthetic strategy uses a "nonconventional" method, initially developed to prepare high surface area porous materials, to introduce true mesoporosity into the PMMA void spaces, without the use of any additional template or matrix.

Looking forward, it is expected that these 3DOM structures could be employed as sensors, catalysts, porous electrodes, or as well mediators in a host of other interesting applications within the materials science community.

ASSOCIATED CONTENT

Supporting Information

TGA/drTGA profiles, additional SEM images of the poly(methyl methacrylate) templates, as well as high-magnification SEM images of 3DOM materials. This material is available free of charge via the Internet at http://pubs.acs.org.

AUTHOR INFORMATION

Corresponding Author

*E-mail: louisa.hope-weeks@ttu.edu.

Notes

The authors declare no competing financial interest.

ACKNOWLEDGMENTS

This material is based upon work supported by the U.S. Department of Homeland Security under Award Number 2008-ST-061-ED0001. The views and conclusions contained in this document are those of the authors and should not be interpreted as necessarily representing the official policies, either expressed or implied, of the U.S. Department of Homeland Security. The authors would also like to personally thank Dr. Fernando Hung Low and Sanjoy Bhattacharia for assistance with data collection and helpful discussions on the research.

REFERENCES

(1) Umeda, G. A.; Chueh, W. C.; Noailles, L.; Haile, S. M.; Dunn, B. S. *Energy Environ. Sci.* **2008**, *1*, 484−486.
(2) Holland, B. T.; Blandford, C. F.; Stein, A. *Science* **1998**, *281*, 538−540.
(3) Holland, B. T.; Blandford, C. F.; Stein, A. *Science* **1999**, *11*, 795−805.
(4) Schroden, R. C.; Al-Daous, M.; Blandford, C. F.; Stein, A. *Chem. Mater.* **2002**, *14*, 3305−3315.
(5) Li, H.; Zhang, L.; Dai, H.; He, H. *Inorg. Chem.* **2009**, *48*, 4421−4434.
(6) Schroden, R. C.; Stein, A. *3D Ordered Macroporous Materials, Colloid Assemblies*; Caruso, F., Ed.; Wiley-VCH Verlag GmbH and Co. KGaA: Weinheim, Germany, 2004; p 465.
(7) D'Arienzo, M.; Armelao, L.; Mari, C. M.; Polizzi, S.; Ruffo, R.; Scotti, R.; Morazzoni, F. *J. Am. Chem. Soc.* **2011**, *133*, 5296−5304.
(8) Petkovich, N. D.; Stein, A. *Colloidal Crystal Templating Approaches to Materials with Hierarchical Porosity, Hierarchically Structured Porous Materials*; Su, B. L., Sanchez, C., Yang, X. Y., Ed.; Wiley-VCH Verlag GmbH and Co. KGaA: Weinheim, Germany, 2012; p 55.
(9) Malic, B.; Kosec, M.; Arcon, I.; Kodre, A. *J. Eur. Ceram. Soc.* **2005**, *25*, 2241−2246.
(10) Yan, H.; Blandford, C. F.; Holland, B. T.; Smyrl, W. H.; Stein, A. *Chem. Mater.* **2000**, *12*, 1134−1141.
(11) Yan, H.; Blandford, C. F.; Lytle, J. C.; Smyrl, W. H.; Stein, A. *Chem. Mater.* **2001**, *13*, 4314−4321.
(12) Sadakane, M.; Asanuma, T.; Kubo, J.; Ueda, W. *Chem. Mater.* **2005**, *17*, 3546−3551.
(13) Sadakane, M.; Horiuchi, T.; Kato, N.; Takahashi, C.; Ueda, W. *Chem. Mater.* **2007**, *19*, 5779−5785.
(14) Sadakane, M.; Sasaki, K.; Nakamura, H.; Yamamoto, T.; Ninomiya, W.; Ueda, W. *Langmuir* **2012**, *28*, 17766−17770.
(15) Zhang, R.; Dai, H.; Du, Y.; Zhang, L.; Deng, J.; Zia, Y.; Zhao, Z.; Meng, X.; Liu, Y. *Inorg. Chem.* **2011**, *50*, 2534−2544.
(16) Yan, H.; Blandford, C. F.; Holland, B. T.; Parent, M.; Smyrl, W. H.; Stein, A. *Adv. Mater.* **1999**, *11*, 1003−1006.
(17) Yan, H.; Blandford, C. F.; Smyrl, W. H.; Stein, A. *Chem. Comm* **2000**, 1477−1478.
(18) Blandford, C. F.; Schroden, R. C.; Al-Daous, M.; Stein, A. *Adv. Mater.* **2001**, *13*, 26−29.
(19) Stein, A.; Li, F.; Denny, N. R. *Chem. Mater.* **2008**, *20*, 649−666.
(20) Brown, P. D.; Gill, S. K.; Hope-Weeks, L. J. *J. Mater. Chem.* **2011**, *21*, 4204−4208.
(21) Davis, M.; Gümeci, C.; Black, B.; Korzeniewski, C.; Hope-Weeks, L. J. *RSC Adv.* **2012**, *2*, 2061−2066.
(22) Gao, Y. P.; Sisk, C. N.; Hope-Weeks, L. J. *Chem. Mater.* **2007**, *19*, 6007−6011.
(23) Gash, A. E.; Satcher, J. H., Jr.; Simpson, R. L. *J. Non-Cryst. Solids* **2004**, *350*, 145−151. Baumann, T. F.; Gash, A. E.; Chinn
(24) Sawvel, S. C.; Maxwell, A. M.; Satcher, J.H., R. S., Jr. *Chem. Mater.* **2005**, *17*, 395−401.
(25) Sisk, C. N.; Hope-Weeks, L. J. *J. Mater. Chem.* **2008**, *18*, 2607−2610.
(26) Kido, Y.; Nakanishi, K.; Miyasaka, A.; Kanamori, K. *Chem. Mater.* **2012**, *24*, 2071−2077.
(27) Gash, A. E.; Tillotson, T. M.; Satcher, J. H., Jr.; Hrubesh, L. W.; Simpson, R. L. *J. Non-Cryst. Solids* **2001**, *285*, 22−28.
(28) Gash, A. E.; Tillotson, T. M.; Satcher, J. H., Jr.; Poco, J. F.; Hrubesh, L. W.; Simpson, R. L. *Chem. Mater.* **2001**, *13*, 999−1007.
(29) Tokudome, Y.; Fujita, K.; Nakanishi, K.; Miura, K.; Hirao, K. *Chem. Mater.* **2007**, *19*, 3393−3398.
(30) Clapsaddle, B. J.; Sprehn, D. W.; Gash, A. E.; Satcher, J. H., Jr.; Simpson, R. L. *J. Non-Cryst. Solids* **2004**, *350*, 173−181.
(31) Tillotson, T. M.; Gash, A. E.; Simpson, R. L.; Hrubesh, L. W.; Satcher, J. H., Jr; Poco, J. F. *J. Non-Cryst. Solids* **2001**, *285*, 338−345.

(32) Long, J. W.; Logan, M. S.; Rhodes, C. P.; Carpenter, E. E.; Stroud, R. M.; Rolison, D. R. *J. Am. Chem. Soc.* **2004**, *126*, 16879−16889.
(33) Bali, S.; Huggins, F. E.; Huffman, G. P.; Ernst, R. D.; Pugmire, R. J.; Eyring, E. M. *Energy Fuels* **2008**, *23*, 14−18.
(34) Chervin, C. N.; Clapsaddle, B. J.; Chiu, H. W.; Gash, A. E.; Satcher, J. H., Jr.; Kauzlarich, S. M. *Chem. Mater.* **2006**, *18*, 4865−4874.
(35) Leventis, N.; Vassilaras, P.; Fabrizio, E. F.; Dass, A. *J. Mater. Chem.* **2007**, *17*, 1502−1508.
(36) Pettigrew, K. A.; Long, J. W.; Carpenter, E. E.; Baker, C. C.; Lytle, J. C.; Chervin, C. N.; Logan, M. S.; Stroud, R. M.; Rolison, D. R. *ACS Nano* **2008**, *2* (4), 784−790.
(37) Davis, M.; Zhang, K.; Wang, S.; Hope-Weeks, L. J. *J. Mater. Chem.* **2012**, *22*, 20163−20165.
(38) Wu, Q. Z.; Yi, Q.; Liao, J. F.; Deng, J. H.; Li, Y. G. *Acta Chim. Sin.* **2005**, *63*, 891−896.
(39) Davis, M.; Hikal, W. M.; Gümeci, C.; Hope-Weeks, L. J. *Catal. Sci. Technol.* **2012**, *2*, 922−924.
(40) Chervin, C. N.; Clapsaddle, B. J.; Chiu, H. W.; Gash, A. E.; Satcher, J. H., Jr.; Kauzlarich, S. M. *Chem. Mater.* **2005**, *17*, 3345−3351.
(41) Stroud, R. M.; Deoscher, M. S.; Rolison, D. R. *Chem. Mater.* **2006**, *18*, 50−58.